EPJ Web of Conferences **276**, 01015 (2023) https://doi.org/10.1051/epjconf/202327601015
SQM 2022

Phase diagram of the QCD Kondo effect and inactivation of the magnetic catalysis

Koichi Hattori[1,2], *Daiki* Suenaga[2,3], *Kei* Suzuki[4], and *Shigehiro* Yasui[5]

[1]Zhejiang Institute of Modern Physics, Department of Physics, Zhejiang University, Hangzhou, 310027, China

[2]Research Center for Nuclear Physics (RCNP), Osaka University, Osaka 567-0047, Japan

[3]Strangeness Nuclear Physics Laboratory, RIKEN Nishina Center, Wako 351-0198, Japan

[4]Advanced Science Research Center, Japan Atomic Energy Agency (JAEA), Tokai 319-1195, Japan

[5]Research and Education Center for Natural Sciences, Keio University, Hiyoshi 4-1-1, Yokohama, Kanagawa 223-8521, Japan

Abstract. We investigate the QCD phase diagram in strong magnetic fields with heavy-quark impurities and determine the ground state within the mean-field analysis. The ground state is characterized by magnitudes of the pairing not only between the light quark and antiquark, i.e., chiral condensate, but also between the light quark and heavy-quark impurity, dubbed the Kondo condensate. We propose signatures of the interplay and/or competition between those two pairing phenomena reflected in the magnitude of the chiral condensate that is saturated with respect to the magnetic-field strength and anomalously increases with increasing temperature.

1 Introduction

Magnetic fields restrict motion of charged particles within the cyclotron orbits, and reduce the dimension of the phase space occupied by the low-energy particles. Pairing among the particles is enhanced in the dimensionally reduced systems. Two of such effects are the quark-antiquark pairing, i.e., chiral condensate, and the pairing between a light quark and heavy-quark impurity dubbed the Kondo condensate. It is important to note that the pairing occurs only for the dimensional reason no matter how small the interaction strength is: The occurrence of the pairing is inevitable when the magnetic-field strength is larger than the temperature scale. The former pairing has been intensively studied under the name of the magnetic catalysis [1] (see, e.g., Ref. [2] for a review), while the latter is proposed as the novel Kondo effect induced by background magnetic fields [3] particularly in QCD (which is analogous to that in finite-density QCD [4, 5]). We investigate interplay and competition between these two pairing phenomena that enrich the phase diagram in strong magnetic fields.

2 Formalism

We discuss the essence of the chiral symmetry breaking and the Kondo effect in magnetic fields with a four-Fermi interaction model [6] (see also Ref. [7])

$$\begin{aligned}\mathcal{L} &= \bar{\psi}(i\partial\!\!\!/_{\parallel} - m_l)\psi + \frac{G_{ll}}{2N}\left[(\bar{\psi}\psi)^2 + (\bar{\psi}i\gamma_5\psi)^2\right] \\ &\quad + \sum_{c=\pm}\Big[\, c\bar{\Psi}_v^c i\partial_0\Psi_v^c + \frac{G_{hl}}{N}\left\{(\bar{\psi}\Psi_v^c)(\bar{\Psi}_v^c\psi) + (\bar{\psi}i\gamma_5\Psi_v^c)(\bar{\Psi}_v^c i\gamma_5\psi)\right\}\Big], \end{aligned} \tag{1}$$

where we have the number of colors $N = 3$, light-quark mass m_l, and the coupling strengths G_{hl} and G_{ll} for the interactions between the heavy and light quarks and between the light quarks, respectively. The light quark ψ in the lowest Landau level (LLL) has the dimensionally reduced kinetic term with $\partial\!\!\!/_{\parallel} = \gamma^0\partial_0 + \gamma^3\partial_3$ when the magnetic field is applied in the spatial third direction. Ψ_v^+ and Ψ_v^- are the heavy-fermion and its antifermion fields introduced as impurities. We took the leading-order terms in the heavy-quark expansion with respect to the inverse mass.

We introduce the chiral condensate $\langle\bar{\psi}\psi\rangle_{\rm LLL} \equiv -\frac{N}{G_{ll}}M$, and the Kondo condensate $\langle\bar{\psi}\Psi_v^{\pm}\rangle_{\rm LLL} \equiv \frac{N}{G_{hl}}\Delta$. In this work, we assume only the color-singlet condensates which are the dominant ones among all the color channels in the large N_c limit (see Ref. [8]). We then determine the magnitudes of those condensates self-consistently from the global minimum of the effective potential. At the linear order in the fluctuations around the mean fields, one can diagonalize the Lagrangian (1) to find four eigenvalues [6]

$$E_{\pm}(p_z) \equiv \pm\frac{1}{2}\left(\sqrt{E_{p_z}^2 + |2\Delta|^2} \pm E_{p_z}\right), \quad \tilde{E}_{\pm}(p_z) \equiv \pm\frac{1}{2}\left(\sqrt{E_{p_z}^2 + |2\Delta|^2} \mp E_{p_z}\right), \tag{2}$$

where $E_{p_z} \equiv \sqrt{p_z^2 + (m_l + M)^2}$. The thermodynamic potential is then written down as [6]

$$\tilde{\Omega}(M,\Delta) = \frac{1}{2\tilde{G}_{ll}}M^2 + \frac{1}{2\tilde{G}_{hl}}|2\Delta|^2 - \sum_i\int_{-\Lambda}^{\Lambda}\frac{dp_z}{2\pi}\frac{1}{2}|\mathcal{E}_i| - \sum_i\int_{-\infty}^{\infty}\frac{dp_z}{2\pi}\frac{1}{\beta}\ln\left(1 + e^{-\beta|\mathcal{E}_i|}\right), \tag{3}$$

where the last term is for the finite-temperature contribution with the inverse temperature $\beta = 1/T$. The sum runs over the four eigenmodes $\mathcal{E}_i = \{E_+, E_-, \tilde{E}_+, \tilde{E}_-\}$. Here, we have introduced normalized quantities $\tilde{\Omega} = \Omega/(N\rho_B)$, $\tilde{G}_{hl} = \rho_B G_{hl}$, and $\tilde{G}_{ll} = \rho_B G_{ll}$ with the Landau degeneracy factor $\rho_B = |q_l B|/(2\pi)$ that stems from the momentum integral over the degenerate two-dimensional phase space. As a result, we are left with the thermodynamic potential with the one-dimensional momentum integral. Λ is the momentum cutoff that may be determined by fitting physical quantities with the lattice QCD data in magnetic fields.

3 Zero-temperature results

By minimizing the thermodynamic potential, we determine the ground state. The numerical results at zero temperature are shown in the left panel of Fig. 1. The Kondo condensate is shown with the blue lines. The dotted and dashed lines show the Kondo condensate at zero and nonzero light quark mass m_l, respectively, when the chiral condensate is absent or formally $G_{ll} = 0$. While there is no phase transition at $m_l = 0$, a finite m_l changes it to a phase transition at a critical magnetic-field strength B_{cK}. Thus, the light-quark mass plays an important role for the Kondo effect.

The solid blue line shows the full result in the presence of competition with the chiral condensate at $G_{ll}\Lambda^2 = 1.0$ and $G_{hl}\Lambda^2 = 3.0$. We find a up-shift of the critical magnetic-field

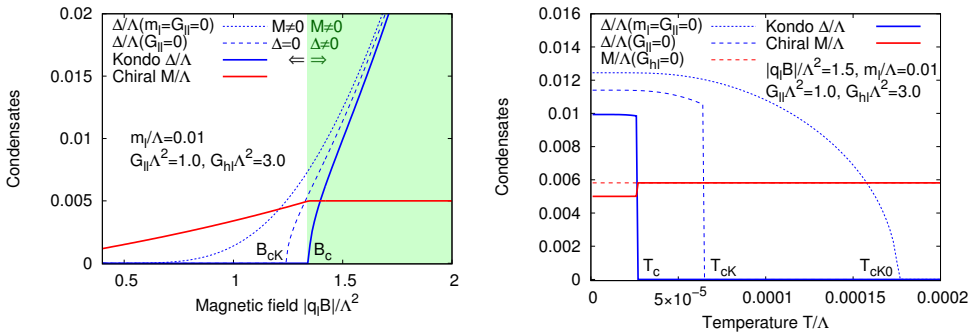

Figure 1. Magnitudes of the chiral and Kondo condensates at zero temperature (left) and at finite temperature (right) [6]. The solid lines show the full results with nonzero G_{hl} and G_{ll}, while the dotted and dashed lines show the results with the competition turned off with either $G_{ll} = 0$ or $G_{ll} = 0$.

strength to B_c, indicating that the Kondo effect is prohibited by the existence of the chiral condensate in the regime between B_{cK} and B_c. However, once the Kondo condensate appears at B_c, the chiral condensate, shown with the red line, saturates at a constant value. Such a *saturation of the chiral condensate* serves as a clear signal of the emergence of the Kondo condensate since it has been known that the chiral condensate monotonically increases by the magnetic catalysis [1] if the heavy-quark impurity is absent or formally $G_{hl} = 0$. Due to this saturation, the Kondo condensate eventually overwhelms the chiral condensate.

One can confirm those findings with analytic solutions to the gap equations [6]

$$\frac{M}{\tilde{G}_{ll}} + \frac{M+m_l}{2\pi}\ln\Xi = 0, \quad \frac{\Delta}{\tilde{G}_{hl}} + \frac{\Delta}{2\pi}\ln\Xi = 0, \tag{4}$$

with $\Xi = \frac{(M+m_l)^2+4|\Delta|^2}{\left(\Lambda+\sqrt{(M+m_l)^2+4|\Delta|^2+\Lambda^2}\right)^2}$. They are derived from the stationary conditions $\partial\tilde{\Omega}/\partial M = 0 = \partial\tilde{\Omega}/\partial\Delta$. We immediately notice that the gap equations (4) have a trivial solution $\Delta = 0$ and a nontrivial solution M, indicating the prohibition of the Kondo condensate. This is the set of solutions below B_c which we call $(M_1, \Delta_1 = 0)$. By eliminating $\ln\Xi$ in Eq. (4), one can find another set of solutions (M_2, Δ_2) as [6]

$$M_2 = \frac{m_l G_{ll}}{G_{hl} - G_{ll}}, \quad \Delta_2 = \frac{1}{2}\sqrt{\frac{\Lambda^2}{\sinh^2(2\pi^2/\tilde{G}_{hl})} - \frac{m_l^2 G_{hl}^2}{(G_{hl}-G_{ll})^2}}\,. \tag{5}$$

By solving $\Delta_2 = 0$, we obtain the critical magnetic-field strength [6]

$$q_l B_c = \frac{4\pi^3}{G_{hl}\,\mathrm{arcsinh}\left(\Lambda\frac{|G_{hl}-G_{ll}|}{m_l G_{hl}}\right)} \sim \frac{4\pi^3 m_l}{\Lambda|G_{hl}-G_{ll}|}, \tag{6}$$

where the last expression holds for a small value of $|G_{hl} - G_{ll}|$. The true vacuum switches over from $(M_1, \Delta_1 = 0)$ to (M_2, Δ_2) at B_c. The second set of solutions indicates the coexistence phase of both the condensates observed above B_c in Fig. 1, where the chiral condensate is saturated with the constant value M_2. Taking the cutoff scale Λ of the order of several hundred MeV, the above critical magnetic field is estimated to be sevelral GeV^2. This strength may be larger than those realized in LHC and RHIC, but are comparable to those that have been realized in recent lattice QCD simulations [9].

4 Finite-temperature results

Finally, we investigate the phase diagram at finite temperature and in strong magnetic fields. In the right panel of Fig. 1, we show the numerical results of temperature dependence of the condensates with the magnetic-field strength and the heavy-light coupling fixed at $|q_l B|/\Lambda^2 = 1.5$ and $G_{hl}\Lambda^2 = 3.0$. The Kondo condensate at $G_{ll} = 0$ and in the chiral limit ($m_l = 0$) is shown with the blue dotted line. We find a phase transition at the critical temperature T_{cK0}. When we switch on a light-quark mass $m_l/\Lambda = 0.01$, as shown by the blue dashed line, the magnitude of condensate is slightly suppressed, and the critical temperature decreases to T_{cK}. This m_l dependence is consistent with our result at zero temperature.

We now consider the chiral condensate with nonzero G_{ll}. First, without the competition at $G_{hl} = 0$, the chiral condensate M, shown with the red dashed line, is almost flat within the plot range and decreases at higher temperature. This is the result with the magnetic catalysis. The chiral condensate at nonzero m_l shows a crossover transition, and its pseudocritical temperature is located even in the higher-temperature region.

The full numerical results including both nonzero G_{ll} and G_{hl} are shown by the solid lines. We find that the chiral and Kondo condensates coexist at low temperature below T_c. Here, the critical temperature T_c for the Kondo condensate decreases from T_{cK} due to the competition effect. It is remarkable that the chiral condensate *increases abruptly* just above T_c to merge to the value in the absence of the competition. This anomalous increase with increasing temperature signals the end of competition and serves as an indirect evidence of the Kondo condensate below T_c even if measurement of the Kondo condensate itself is tough. There is no competition above T_c, and the chiral condensate never increases as we further increase temperature.

5 Conclusion and outlook

We reported the novel phase diagram emerging from the competition between the chiral and Kondo condensates in strong magnetic fields. At low temperature, the competition causes a *saturation behavior* of the chiral condensate above the critical magnetic-field strength. At finite temperature, the competition leads to a *steep increase* of the chiral condensate just above the critical temperature for the Kondo condensate. This anomalous increasing behavior signals the end of the competition. Our findings shed light on the intertwined dynamics with light and heavy quarks and may stimulate further developments of the nonperturbative many-body phenomena and of the lattice simulations in strong magnetic fields.

In fact, lattice QCD simulations in strong magnetic fields elucidated the magnetic catalysis in QCD with high precision, and they can be also applied to the counterpart in solid-state physics. The magnetically induced Kondo effect will be also confirmed by direct measurements of the Kondo condensate constructed from the correlation function of the heavy and light fermions or by indirect ones via the characteristic behaviors of the chiral condensate.

Acknowledgement.—This work was supported by Japan Society for the Promotion of Science (JSPS) KAKENHI under grant Nos. JP17K14277, JP20K14476, 20K03948, and 22H02316.

References

[1] V. P. Gusynin, V. A. Miransky, I.A. Shovkovy, Phys. Lett. B **349**, 477 (1995), hep-ph/9412257.
[2] I. A. Shovkovy, Lect. Notes Phys. **871**, 13 (2013), 1207.5081.

[3] S. Ozaki, K. Itakura, Y. Kuramoto, Phys. Rev. D **94**, 074013 (2016), 1509.06966.
[4] S. Yasui, K. Sudoh, Phys. Rev. C **88**, 015201 (2013), 1301.6830.
[5] K. Hattori, K. Itakura, S. Ozaki, S. Yasui, Phys. Rev. D **92**, 065003 (2015), 1504.07619.
[6] K. Hattori, D. Suenaga, K. Suzuki, S. Yasui, *in preparation*.
[7] Y. Araki, D. Suenaga, K. Suzuki, S. Yasui, Phys. Rev. Research **3**, 013233 (2021), 2008.08434.
[8] S. Yasui, K. Suzuki, and K. Itakura, Nucl. Phys. A **983**, 90–102 (2019), 1604.07208; S. Yasui, Phys. Lett. B **773**, 428–434 (2017), 1608.06450; S. Yasui, K. Suzuki, and K. Itakura, Phys. Rev. D **96**, 014016 (2017), 1703.04124.
[9] G. Endrődi, JHEP **07**, 173 (2015), 1504.08280; M. D'Elia, et al., Phys. Rev. D **105**, 034511 (2022), 2111.11237.